Biophysical Journal Volume 93 October 2007 2969–2977

Characterization of the Threshold Response of Initiation of Blood Clotting to Stimulus Patch Size

Christian J. Kastrup, Feng Shen, Matthew K. Runyon, and Rustem F. Ismagilov
Department of Chemistry and Institute for Biophysical Dynamics, The University of Chicago, Chicago, Illinois

ABSTRACT This article demonstrates that the threshold response of initiation of blood clotting to the size of a patch of stimulus is a robust phenomenon under a wide range of conditions and follows a simple scaling relationship based on the Damköhler number. Human blood and plasma were exposed to surfaces patterned with patches presenting clotting stimuli using microfluidics. Perturbations of the complex network of hemostasis, including temperature, variations in the concentration of stimulus (tissue factor), and the absence or inhibition of individual components of the network (factor IIa, factor V, factor VIII, and thrombomodulin), did not affect the existence of this response. A scaling relationship between the threshold patch size and the timescale of reaction for clotting was supported in numerical simulations, a simple chemical model system, and experiments with human blood plasma. These results may be useful for understanding the spatiotemporal dynamics of other autocatalytic systems and emphasize the relevance of clustering of proteins and lipids in the regulation of signaling processes.

INTRODUCTION

This article describes experiments and numerical simulations to characterize the threshold response of blood clotting to the size of a patch presenting a clotting stimulus. Understanding the dynamics of blood clotting is important to biomedical applications as well as the study of complex networks. The spatiotemporal dynamics of initiation of blood clotting is particularly interesting, as blood clotting must initiate and remain localized at sites of vascular damage, and common clotting disorders are related to the failure of this process. Understanding how initiation of blood clotting is regulated is difficult, as it involves simultaneous consideration of the entire complex network of clotting reactions as well as the spatial and temporal effects associated with the vascular system.

Numerous experimental and theoretical studies have provided valuable insight into how initiation of clotting is regulated. Transport of activators and inhibitors of clotting by both diffusion and convection (fluid flow) has been proposed to contribute to the regulation of initiation of surface reactions in blood clotting (1–8). Experimental studies have shown that reactions in the clotting network are regulated, in part, by a threshold response to the concentration of activators in solution (9–11). Additional theoretical studies proposed that this threshold may be controlled by transport of activators and influenced by the size of a patch of vascular damage (1,4) as well as the concentrations of stimuli on a patch (3).

Our previous experiments (4) demonstrated that initiation of clotting of pooled platelet-poor plasma (pooled-PPP) displayed a threshold response to the size of a patch presenting a clotting stimulus. In addition, we hypothesized that the threshold patch size necessary to initiate clotting could be quantitatively predicted by a scaling relationship based on the Damköhler number, *Da*, which describes the competition between reaction and diffusion of molecules (12–14). Here, we extend previous work to demonstrate that the threshold response of initiation of clotting to patch size is a robust phenomenon under a wide range of conditions. Our goal was not to reproduce all of the conditions present in vivo, but to test the threshold response against a set of well-defined conditions. In addition, we test a scaling relationship between the critical size of a patch of stimulus needed to initiate clotting and the timescale of reaction for clotting. This scaling relationship was supported in numerical simulations and in experiments with both a nonbiological, chemical system and human blood plasma.

MATERIALS AND METHODS

All solvents and salts used in buffers were purchased from commercial sources and used as received unless otherwise stated.

Poly(dimethylsiloxane) (PDMS, Sylgard Brand 184 Silicone Elastomer Kit) was purchased from Dow Corning (Midland, MI).

1,2-dilauroyl-*sn*-glycero-3-phosphocholine (DLPC), L-α-phosphatidylserine from porcine brain, 1,2-dipalmitoyl-*sn*-glycero-3-phosphocholine (DPPC), and 1,2-dimyristoyl-*sn*-glycero-3-phosphocholine (DMPC) were purchased from Avanti Polar Lipids, (Alabaster, AL).

Texas Red 1,2-dihexadecanoyl-*sn*-glycero-3-phosphoethanolamine (Texas Red DHPE), *n*-(7-nitrobenz-2-oxa-1,3-diazol-4-yl)-1,2-dihexadecanoyl-*sn*-glycero-3-phosphoethanolamine triethylammonium salt (NBD-PE), and rhodamine 110-bis-(p-tosyl-L-glycyl-L-prolyl-L-arginine amide) were purchased from Molecular Probes/Invitrogen (Eugene, OR).

T-butyloxycarbonyl-β-benzyl-L-aspartyl-L-prolyl-L-arginine-4-methylcoumaryl-7-amide (Boc-Asp(OBzl)-Pro-Arg-MCA) and t-butyloxycarbonyl-Leu-Ser-Thr-Arg-4-methylcoumaryl-7-amide (Boc-Leu-Ser-Thr-Arg-MCA) were purchased from Peptides International (Louisville, KY).

Albumin from bovine serum, alginic acid, and 2-nitrobenzaldehyde were purchased from Sigma (St. Louis, MO).

Argatroban was obtained from GlaxoSmithKline (Research Triangle Park, NC).

Submitted March 29, 2007, and accepted for publication June 12, 2007.

Address reprint requests to R. F. Ismagilov, Tel.: 773-702-5816; E-mail: r-ismagilov@uchicago.edu.

Editor: Raimond L. Winslow.

0006-3495/07/10/2969/09 $2.00

doi: 10.1529/biophysj.107.109009

Human recombinant tissue factor (TF), human thrombin, and corn trypsin inhibitor were purchased from Calbiochem/EMB Biosciences (La Jolla, CA).

Rabbit lung thrombomodulin (TM) and human protein C were obtained from American Diagnostica (Stamford, CT).

Bromophenol blue and sodium chlorite ($NaClO_2$, 80% purity) were purchased from Acros Organics (Morris Plains, NJ).

Krytox fluorinated grease is a product of Dupont (Wilmington, DE).

Sodium thiosulfate ($Na_2S_2O_3$, 99.9% purity) and anhydrous methyl sulfoxide (DMSO, 99.7% purity) were purchased from Fisher Scientific (Fair Lawn, NJ).

Dimethylsiloxane-ethylene oxide block copolymer was purchased from Gelest (Morrisville, PA).

Siliconized coverslips were obtained from Hampton Research (Aliso Viejo, CA).

Normal pooled plasma (human, platelet poor) was purchased from George King Bio-Medical (Overland Park, KS).

Human whole blood was obtained from individual healthy donors in accordance with the guidelines set by the Institutional Review Board (protocol # 12502A) at The University of Chicago.

Generating patches of tissue factor (TF) surrounded by an inert phospholipid bilayer

The methods used here to prepare lipid vesicles and bilayers have been previously described (4). The inert lipid bilayer contained 97 mol % of DPPC and 3% of a green fluorescent dye (NBD-PE) (4). In experiments with TM reconstituted into the lipid bilayer, the inert bilayer consisted of a lipid mixture of DMPC (48.5%), DPPC (48.5%), and 3% NBD-PE, and contained thrombomodulin (TM) at a calculated concentration of 40 pmol/m^2 (actual ratio of TM/lipids $= 1.3 \times 10^{-5}$). TM was incorporated into vesicles as previously described (15).

In the control experiment to determine the activity of TM in the phospholipid bilayer, the rate of protein C activation in the presence of thrombin was measured (16). A function of TM is to convert protein C to activated protein C (APC) when thrombin binds to TM (17,18). The concentration of APC was determined using an APC-sensitive fluorogenic peptide dye, Boc-Leu-Ser-Thr-Arg-MCA (19). A solution containing 0.1 mM of the fluorogenic peptide dye, 5 nM human thrombin, 800 nM human protein C, 0.1% bovine serum albumin, 5 mM $CaCl_2$, 20 mM TRIS, and 100 mM NaCl (final pH 7.5) was prepared and immediately placed in contact with the phospholipid bilayer reconstituted with TM. The blue fluorescence intensity was measured every 5 min for up to 3 h. The sample was stirred gently between measurements. APC production was determined based on Michaelis-Menten kinetics and known kinetics for the APC fluorogenic dye (19). Thrombin is known to activate protein C directly and to slowly activate the APC fluorogenic dye. Thus, the background fluorescence, measured in control samples containing no TM, was subtracted from the measured fluorescence intensity in samples containing TM. For a bilayer containing a calculated TM concentration of 40 pmol/m^2, APC production was 35 pmol/min/m^2, which is on the same order of magnitude as previously measured for a monolayer of endothelial cells (20).

A photomask patterned with circular patches of different sizes was placed over the inert bilayer and irradiated with deep UV light. The patterned bilayer was backfilled with vesicles containing 79.5 mol % of DLPC, 20 mol % of porcine brain, 0.5 mol % of a red fluorescent dye (Texas Red DHPE), and TF (concentrations between 0.3 and 8 pmol/m^2).

Measuring initiation time of human blood and plasma on patches of TF

Pooled platelet-poor plasma (pooled-PPP) was used as received from the commercial source. Whole blood obtained from donors was collected in Vacutainer tubes (Becton-Dickinson, Franklin Lakes, NJ) containing 3.2% sodium citrate (9:1 by volume). Platelet-rich plasma (PRP) was obtained by centrifuging whole blood at 300 *g* for 10 min. PPP was obtained by centrifuging whole blood at 800 *g* for 10 min, then centrifuging the plasma again at 800 *g* for 10 min. All blood and plasma were incubated with corn trypsin inhibitor (100 μg/mL) to inhibit the factor XII pathway of initiation of clotting (21). Citrated pooled-PPP, PRP, and PPP (300 μL) were recalcified by adding a solution of $CaCl_2$ containing a thrombin-sensitive fluorescent substrate, Boc-Asp(OBzl)-Pro-Arg-MCA (100 μL, 40 mM $CaCl_2$, 90 mM NaCl, and 0.4 mM Boc-Asp(OBzl)-Pro-Arg-MCA). Argatroban was added to the pooled-PPP at desired concentrations of 0 to 2.5 μg/mL. To recalcify whole blood (22), the whole blood (376 μL) was mixed with a thrombin-sensitive fluorescent substrate, rhodamine 110-bis-(p-tosyl-L-glycyl-L-prolyl-L-arginine amide) (2 μL, 10 mM in DMSO), and then added to a solution of $CaCl_2$ (23.5 μL, 200 mM). Recalcified whole blood or plasma (400 μl) was placed in contact with the patterned bilayer substrate in a microfluidic chamber (4). Initiation of clotting was measured by monitoring the formation of thrombin and fibrin. The formation of thrombin was monitored by fluorescence microscopy to detect the cleavage products from the thrombin-sensitive fluorescent substrates. The formation of fibrin was detected using bright-field microscopy.

Measuring initiation time of the nonbiological, chemical system on patches of acid

The reaction solution in the nonbiological, chemical system was composed of equal parts of two precursor aqueous solutions: 1), sodium thiosulfate ($Na_2S_2O_3$, 0.492mmol), alginic acid (5.8 mg/mL), and bromophenol blue (0.425 mM) with a final pH 7; and 2), sodium chlorite ($NaClO_2$, 2.99 mmol, pH 10.7) (7,23). The photoacid-coated substrate was prepared by spin-coating a siliconized coverslip with a 20–30 μm thick layer of 2-nitrobenzaldehyde (50% by weight) in dimethylsiloxane-ethylene oxide block copolymer. The reaction solution was placed in contact with the photoacid substrate in a microfluidic chamber (4). UV light (300–400 nm) was irradiated on a photomask (CAD Art Services, Bandon, OR) and passed through clear patches to generate H^+ only in specific areas. Initiation of the chemical system was measured by monitoring the fluorescence of bromophenol blue, a pH-sensitive dye, by fluorescence microscopy.

Fabricating the microfluidic chambers

The microfluidic chambers used in the blood and plasma experiments were prepared from PDMS cured on multilevel, machine-milled brass masters. Disposable devices were generated with an inner diameter of 13 mm, an outer diameter of 20 mm, and a depth of 1 mm. The microfluidic chamber used in the nonbiological, chemical system experiment consisted of a PDMS gasket with an inner diameter of 10 mm, an outer diameter of 20 mm, and a depth of 1 mm. The gasket was sealed to a siliconized coverslip and to the photoacid-coated substrate.

Analysis of fluorescence images

Image analysis was preformed as previously described (4). The original gray-scale fluorescence images were collected and false-colored using MetaMorph software (Molecular Devices, Sunnyvale, CA). For each wavelength, the levels were adjusted to the same values. Images were overlaid using Adobe Photoshop software (Adobe, San Jose, CA).

Numerically simulating initiation of an autocatalytic system on different sized patches

Numerical simulations were performed using a commercial finite element package (Comsol Multiphysics 3.2, Comsol, Stockholm, Sweden). Three

rate equations were utilized in the simulation: 1), production of activator, C, at the surface of the patch, rate $= k_{patch,}$; 2), autocatalytic production of C in solution, rate $= k_{prod}[C]^2 + b$ ($k_{prod} = 2 \times 10^7$ M^{-1}/s, $b = 2 \times 10^{-10}$ M/s); and 3), linear consumption of C in solution, rate $= -k_{consum}[C]$ ($k_{consum}[C] = 0.2$ s^{-1}). $k_{patch,}$ was varied from 2.5×10^{-8} to 1×10^{-6} M/s to obtain different values of t_r. The initial concentration of C was 1×10^{-9} M, and the diffusion coefficient was 5×10^{-11} m^2/s. Rate constants were based on known values for reactions in the blood clotting network (5).

RESULTS

Testing the robustness of the threshold response

To test whether the threshold response of clotting on patches is a robust phenomenon, we measured the clot times of human blood and plasma on arrays of patches of varying sizes under a variety of conditions. We used pooled platelet-poor plasma (pooled-PPP), platelet-poor plasma (PPP), platelet-rich plasma (PRP), and whole blood to test the influence of platelets and blood cells on the threshold phenomenon. In addition, we tested the influence of temperature (24 and 37°C) on the threshold response in pooled-PPP and PRP. Using pooled-PPP, we also tested the influence of a membrane-bound inhibitor of clotting, thrombomodulin (TM) (17,18,20, 24), on the threshold response. To determine whether the threshold response was robust in blood from patients with clotting disorders, we tested factor V deficient PPP and factor VIII deficient PPP. We also tested the effect of a factor IIa (thrombin) deficiency on the clotting response by adding argatroban (25), an inhibitor of factor IIa, to pooled-PPP.

Patches consisted of circular areas of a planar phospholipid bilayer (26–28) reconstituted with a clotting stimulus tissue factor (TF) (Fig. 1 *a*) (11,29). Patches were surrounded by an inert phospholipid bilayer (Fig. 1 *b*) (4). For these experiments testing the robustness of the threshold response, the concentration of TF in the phospholipid bilayer was ~0.5 pmol/m^2, but fluctuations in the activity of TF from day to day were observed. To account for slight variations in TF concentration or activity in the phospholipid bilayer between experiments, a control using pooled-PPP was performed for each set of conditions. For experiments testing the influence of TM on the threshold response, TM was reconstituted into the inert phospholipid bilayer (15,30). Clotting was indicated by the appearance of both thrombin and fibrin. The formation of fibrin was monitored by bright-field microscopy, and the formation of thrombin was monitored by fluorescence microscopy, where the concentration of a thrombin-sensitive dye (*blue*) was measured (Fig. 1 *c*) (21,31). Blood plasma was placed on arrays of patches of different sizes, and clot time on each patch was measured. Qualitatively, clotting always occurred on large patches, but not on small patches.

To test the existence of a threshold response, we measured clot time versus patch size for each condition. Clotting of pooled-PPP, PPP, and PRP displayed a threshold response to patch size (Fig. 2, *a–e*). In comparison to pooled-PPP and PPP from a single donor, data from experiments with PRP showed more scatter due to increased spontaneous clotting. Whole blood (Fig. 2 *f*) demonstrated even greater spontaneous clotting, where clotting occurred within 20 min in all experiments, even in experiments with no patches of stimulus. As a result, it was difficult to measure the threshold response in whole blood. While there is a clear transition from slow clotting on patches smaller than 60 μm to faster clotting on patches larger than 80 μm (Fig. 2 *f*), we are hesitant to refer to this transition as a threshold response. To conclusively test whether the threshold dynamics is relevant with whole blood, improvements to the experimental setup are essential, including better control of surface chemistry of microfluidic devices (32–35). Specifically, modification of the bilayer surface by varying lipid composition and membrane protein composition should improve the background clotting time. Additionally, improving the delivery of blood from the patient to the chamber, such as by directly transferring the blood without adding citrate, should improve the experiment. Temperature did not substantially affect the existence of the threshold response in either pooled-PPP (Fig. 2, *a* and *b*) or PRP (Fig. 2, *c* and *d*).

To determine the influence of TM on the threshold response, we monitored clotting of pooled-PPP on patches of TF surrounded by an inert bilayer reconstituted with TM. The calculated TM concentration in the bilayer was

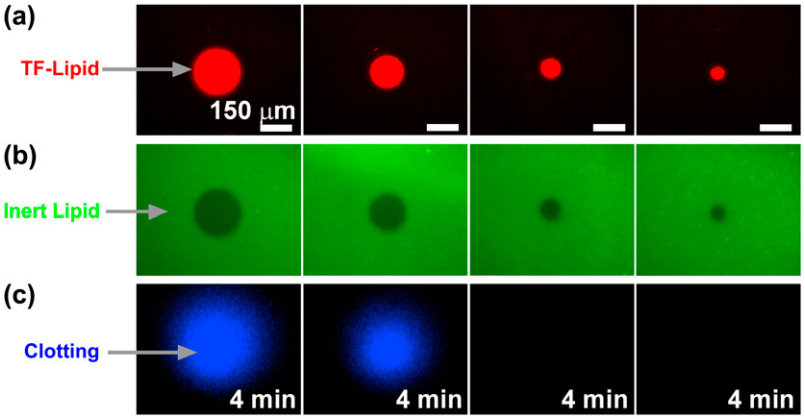

FIGURE 1 Micrographs showing initiation of clotting of platelet-rich plasma on patches of TF reconstituted in a phospholipid bilayer. (*a*) Lipid tagged with red dye was incorporated into a phospholipid bilayer containing phosphatidylcholine, phosphatidylserine, and reconstituted TF. (*b*) Lipid tagged with green dye was incorporated into an inert phospholipid bilayer containing phosphatidylcholine. (*c*) Blue fluorescent dye indicated a high concentration of thrombin, an indicator of clotting. Clotting occurred on patches ≥165 μm, but not on patches ≤90 μm.

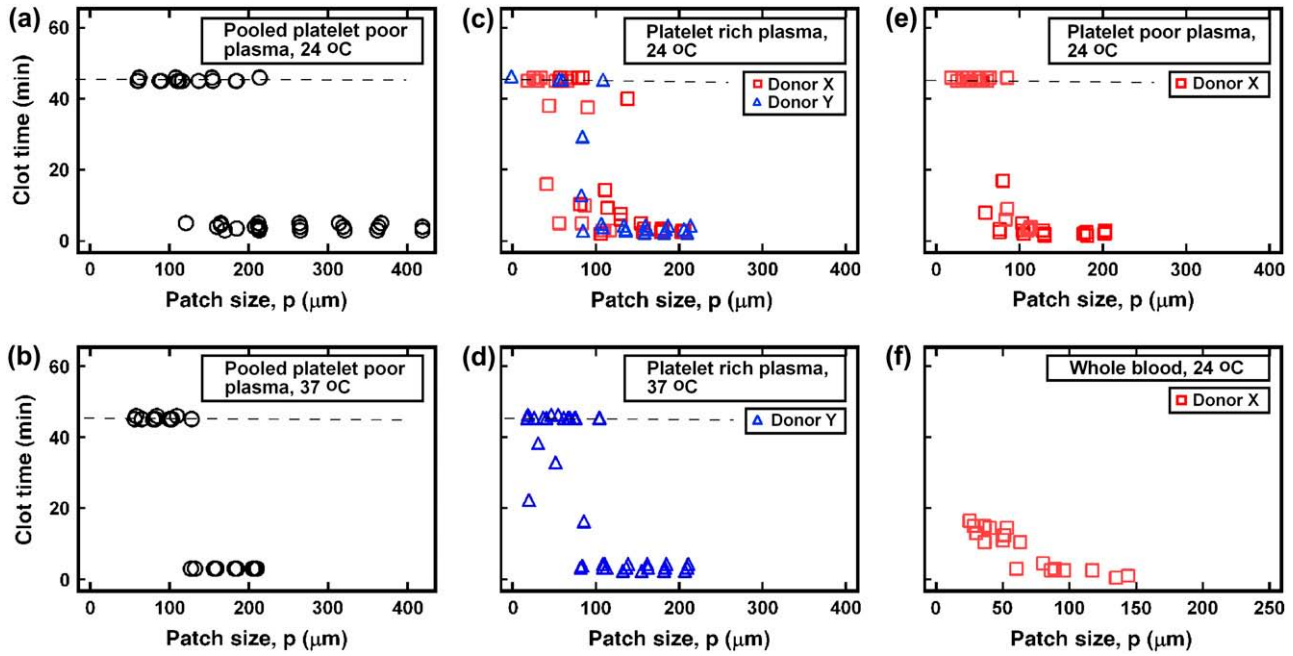

FIGURE 2 Testing the existence of the threshold response of clotting to patch size in several types of human blood plasma and whole blood at 24 and 37°C. Data points on and above the dashed line represent patches that did not clot within 45 min, when the experiments were stopped. Some data points have been shifted above the line to allow for visualization of overlaid data points.

40 pmol/m^2, and control experiments confirmed that TM was active (see Materials and Methods) (16). The presence of TM in the inert bilayer did not affect the existence of the threshold response (Fig. 3). It is has been shown conclusively that TM is a potent anticoagulant in both in vitro and in vivo studies (18,20,24). The inability of TM to prevent clotting on large patches of stimulus in our experiments does not necessarily contradict these studies. In one study, TM was shown to produce activated protein C (APC) with a delay of a few minutes after exposure to thrombin (36). If these results are applicable to our experiments, then inhibition of clotting in the presence of TM would occur after initiation took place. Also, TM in capillaries is believed to be a sink for circulating thrombin, and therefore may act systemically by lowering the steady-state concentration of thrombin. Since our experiments focused on observing the local response, this systemic response would not be detected. Finally, TM is believed to be most important in small capillaries with high surface/volume ratios (18,37). Our experiments have lower surface/volume ratios than capillaries.

PPP deficient in factor V or factor VIII and PPP with partially inhibited factor IIa (thrombin) also displayed a threshold response (Fig. 4). Plasmas deficient in factor V or factor VIII were from human donors with congenial enzyme deficiencies. Argatroban, an inhibitor of factor IIa currently used as an anticoagulant drug, was added directly to pooled-PPP at 1 μg/mL and 2.5 μg/mL to partially inhibit factor IIa. These results show that the existence of the threshold response remains robust even when the concentration of individual components of the hemostasis network is reduced.

Formulating and testing a physical description of the threshold response

We utilized experimentally observable, physical parameters to develop a simplified description of the threshold response.

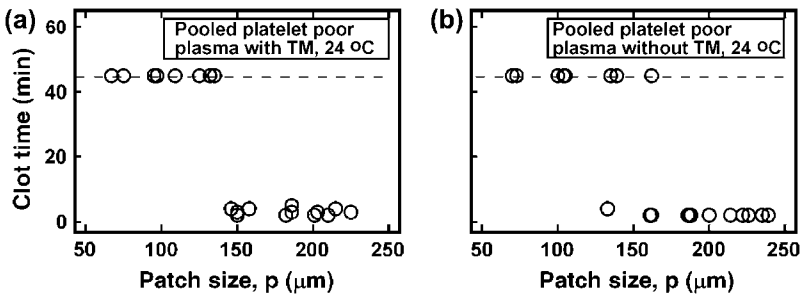

FIGURE 3 Testing the influence of thrombomodulin (TM) on the existence of the threshold response of clotting to patch size. The presence of TM did not affect the existence of the threshold response in pooled-PPP. Data points on the dashed line represent patches that did not clot within 45 min, when the experiments were stopped.

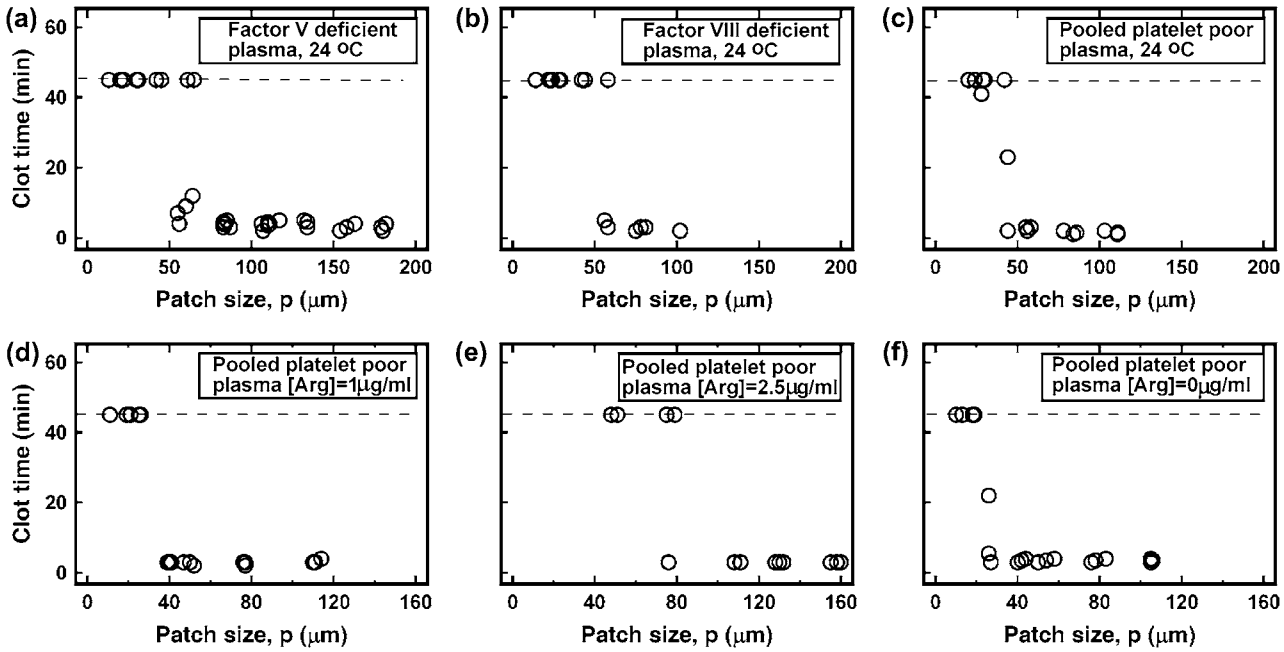

FIGURE 4 Testing the existence of the threshold response of clotting to patch size for plasmas deficient in active clotting enzymes. (*a*,*b*) Pooled-PPP deficient in factor V or factor VIII displayed a threshold response. (*d*,*e*) Pooled-PPP with factor IIa inhibited by argatroban at two different concentrations also displayed a threshold response. The control experiment for panels *a* and *b* is shown in panel *c*, and the control experiment for panels *d* and *e* is shown in panel *f*. Data points on the dashed line represent patches that did not clot within 45 min, when the experiments were stopped.

We previously proposed a scaling relationship based on the Damköhler number to describe initiation of a reaction on patches of surface stimuli (4). The Damköhler number is commonly used to predict the outcome of chemical reactions in systems that include mass transport, based on the competition between reaction and transport (12–14). A threshold response is manifested by the initiation of a reaction only when the concentration of activators exceeds the threshold concentration. Therefore, initiation of a reaction is dependent on competition between the timescale of reaction, t_r, for production of activators on the patch and the timescale of diffusion, t_D, for diffusive transport of activators off the patch (Fig. 5). The magnitude of the Damköhler number, $Da = t_D / t_r$, is dictated by the diameter of the patch, p. Small p corresponds to small t_D and small Da, as diffusion of activators off of the patch occurs rapidly, whereas large p corresponds to large t_D and large Da, as activators take a long time to diffuse away from the patch.

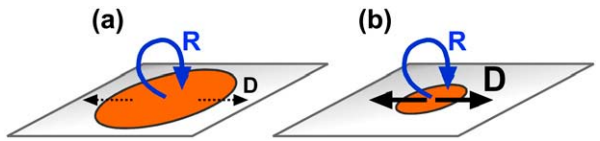

FIGURE 5 Competition between diffusion, D (*black arrows*), and reaction, R (*blue arrows*), of activators determines whether initiation will occur on a given patch (*orange*). The timescale of diffusion is dependent on patch size, whereas the timescale of reaction is independent of patch size. (*a*) When p is large, diffusion is slower than reaction, and initiation occurs. Within the timescale of reaction, diffusion only removes activators from the edge of the patch, allowing a high concentration of activators to accumulate in the center. (*b*) When p is small, diffusion is faster than reaction, and initiation does not occur. Diffusion is able to remove activators from the entire patch before initiation of reaction can occur.

Initiation will occur at large Da when t_r is fast and t_D is slow. Diffusion is described by a simple scaling equation, $t_D \propto p^2/D$, where t_D is the timescale of diffusion [s], p is the patch size [m], and the D is the diffusion coefficient for a particular molecule [m^2/s]. This equation can be used to describe the threshold patch size, p_{tr}, above which initiation occurs. Thus p_{tr} should scale with $t_r^{1/2}$ according to $p_{tr} \propto (D \times t_r)^{1/2}$.

First, we wished to determine whether the scaling prediction was reasonable for a system with diffusion and boundary conditions in three dimensions. To address this question, we used three-dimensional numerical simulations of a simple, autocatalytic system with a threshold response that was activated by patches of stimulus. The rate and diffusion constants used in these simulations were on the same scale as those of known blood clotting components (5). To model an autocatalytic system with a threshold response, two rate equations were incorporated—one that described autocatalytic production of activator, and one that described linear consumption of activator (see Materials and Methods). This type of autocatalytic system was previously proposed to account for the threshold response in the hemostasis network (7,38). These simulations were performed using a commercial software package (Comsol Multiphysics 3.2).

To compare the relationship between p_{tr} and t_r, we first determined the value of t_r for several rates of production from a uniform surface of stimulus. The value of t_r was equal to the initiation time on an infinitely large patch of stimulus with a given rate of production from the surface. Then, we varied p for each t_r to determine p_{tr}. As expected, a threshold patch size existed for each t_r (Fig. 6 *a*), where $p > p_{tr}$ resulted in initiation and growth in three dimensions, and $p < p_{tr}$ did not initiate. A plot of p_{tr} versus t_r showed a one-half power scaling relationship (Fig. 6 *b*) and verified that the scaling prediction was reasonable for systems with three-dimensional diffusion in the presence of realistic boundary conditions resembling those in experiments described above.

Next, we experimentally tested the predicted scaling relationship by using a simple, nonlinear chemical system (7, 23,39–41) composed of three reactions. This chemical system is a simple, autocatalytic system with a threshold response and has been shown to reproduce the nonlinear dynamics of initiation of blood clotting (4,7). Initiation of this autocatalytic system occurs at a critical concentration of activator, the hydronium ion (H_3O^+). Initiation is ''all or nothing,'' corresponding to a switch from basic to acidic conditions and is accompanied by precipitation. In this experiment, patches of acid were selectively produced by irradiating a photoacid layer on the surface through a photomask (4). Different values of t_r were obtained by adjusting the intensity of the irradiation and thus the production of acid from the surface. For each t_r, a specific value of p_{tr} was measured. A plot of p_{tr} versus t_r shows a linear relationship, with a one-half power regression falling within a 97.5% confidence interval of the best fit regression (Fig. 7 *a*), and experimentally supports the scaling prediction.

To demonstrate the applicability of the scaling prediction to complex, biological systems, we tested it by using human pooled-PPP. Initiation of blood clotting occurs at a critical concentration of activators, such as thrombin, and results in autocatalytic production of activators, precipitation of fibrin, and the subsequent formation of a solid clot (11). The stimulus for production of activators in vivo is the enzyme TF. To determine if the scaling prediction applies to blood clotting, we measured the t_r of human blood plasma exposed to surfaces of phospholipid bilayer containing TF in a microfluidic chamber (4). To vary t_r in these experiments, we varied two parameters: 1), the concentration of TF on the surface was varied from 0.3 to 8 pmol/m^2; and 2), the concentration of argatroban, an inhibitor of thrombin, in solution was varied from 0 to 2.5 μg/mL. To measure p_{tr}, patches of TF of specific sizes were created through a photopatterning process (26,27). For each t_r, a specific value of p_{tr} was measured (Fig. 7 *b*).

A plot of p_{tr} versus t_r shows a linear relationship, with a one-half power regression falling within a 97.5% confidence interval of the best fit regression (Fig. 7 *b*). A plot of p_{tr} versus t_r with raw (nonaveraged) data also shows the one-half power regression falling within a 97.5% confidence interval of the best fit regression. As expected for complex biological systems, the amount of scatter in the data was greater in comparison to the numerical simulation and the nonbiological chemical system. Due to this scatter, it is not possible to rule out similar scaling hypotheses. Specifically, it is not possible to rule out a scaling hypothesis with a power of two-thirds, as a two-thirds power regression also falls within a 97.5% confidence interval of the best fit regression. However, it is possible to reject, with >97.5% confidence, the scaling hypotheses with powers of 1 and larger and with powers of one-third and smaller. Thus, at least for this in vitro system, a scaling relationship exits between p_{tr} and t_r, and the scaling power is within a factor of two of that predicted by the chemical model.

DISCUSSION

We have shown that the threshold response of blood clotting to the size of a patch of stimulus is a robust phenomenon under a wide range of conditions. Perturbations of this complex network, such as temperature, variations in the concentration of stimulus, and the absence or inhibition of individual components of the network, did not affect the existence of this response. These studies still do not include many important aspects of coagulation in vivo, and in vivo studies are needed to determine the physiological relevance of these threshold dynamics. Our goal was not to reproduce all of the conditions present in vivo, but to test the threshold response against a set of well-defined conditions. Additional components that may

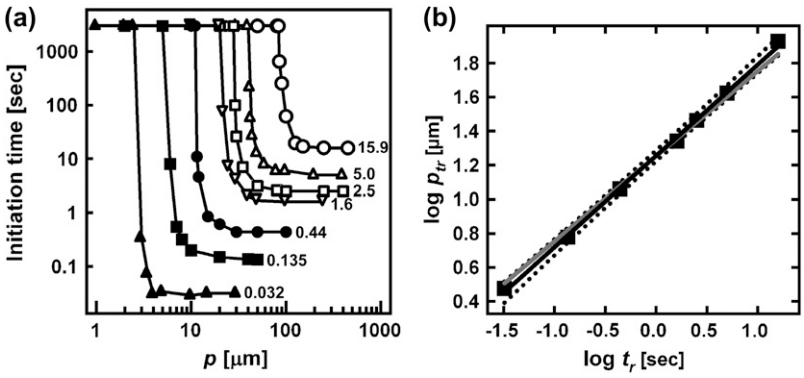

FIGURE 6 Three-dimensional numerical simulations of initiation of clotting show a one-half power scaling relationship between p_{tr} and t_r. (*a*) Initiation time versus p curves show that a specific p_{tr} exists for reach t_r. Each curve corresponds to a particular t_r indicated by the value to the right of the curve (units of seconds), and p_{tr} corresponds to the inflection point of each curve. (*b*) A plot of p_{tr} versus t_r for each curve in panel *a* shows a one-half power scaling relationship. The reference regression, $y = 1/2x + c$ (*shaded*), falls within a 99% confidence limit (*dotted lines*) of the best fit linear regression (*solid*). The slope of the best fit linear regression was 0.54, and the r-value was $r = 0.99$.

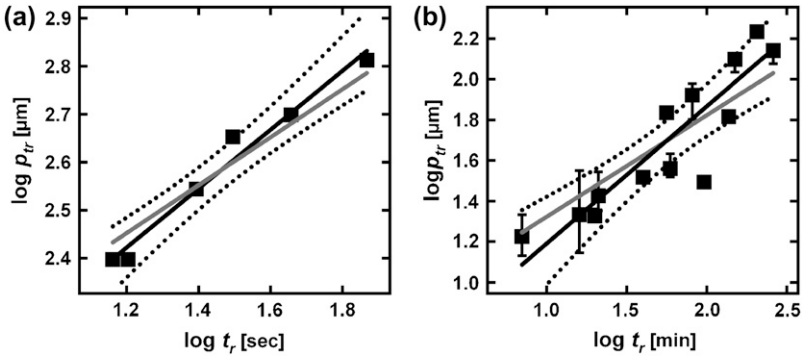

FIGURE 7 Comparing the experiments to the predicted one-half power scaling relationship for (*a*) the simple, nonlinear chemical system and (*b*) the complex system of blood clotting. For both panels *a* and *b*, the reference regression line, $y = 1/2x + c$ (*shaded*), falls within a 97.5% confidence interval (*dotted lines*) of the best fit linear regression (*solid*). The slope of the best fit linear regression was (*a*) 0.61 and (*b*) 0.64. The *r*-value of the best fit linear regression was (*a*) $r = 0.98$ and (*b*) $r = 0.90$. In panel *a*, each data point corresponds to a single experimental value. In panel *b*, each data point for t_r is an average of three values of p_{tr}, except the point $\log t_r = 2.31$, which contains only two values of p_{tr}. Error bars correspond to the maximum and minimum values of p_{tr}.

influence the existence of the threshold response include the presence of cells of the vascular wall and additional three-dimensional microgeometries. While we did not focus on the role of transport by flow in these experiments, flow is certain to affect the threshold response in these systems, as it is known to be important for regulating clotting in vivo. One may expect that flow would act similar to diffusion, removing activators from the patch, leading to larger threshold patch sizes. An important extension of this work would be to test the influence of flow on the threshold patch size. Development of flow chambers with controlled shear (36,42) that are compatible with the lipid patterning techniques (26–28) is a challenge that needs to be addressed. Although not every component involved in hemostasis was tested, the results here show that the threshold is robust for a large range of conditions. These results imply that a mechanism based on physical parameters, not the individual reactions within the network, governs the threshold response, and this mechanism may be fundamental to threshold responses in other autocatalytic systems. These results support our previous assertion that the reactions of the hemostasis network display a modular organization, which may explain the robustness of the threshold response.

To provide a physical description of the threshold response, we predicted a one-half power scaling relationship between the critical size of a patch of stimulus necessary to initiate clotting and the timescale of reaction for clotting. While the one-half power scaling relationship was strongly supported in both a numerical simulation and in experiments with a simple, nonlinear chemical system, experiments with pooled-PPP did not display a scaling relationship of exactly one-half power. It remains to be seen if this discrepancy is due to the difficulty of performing experiments with blood, or due to the higher complexity of blood and its underlying dynamics. Also, in these experiments, the threshold value was measured across almost three orders of magnitude of t_r, and it is possible that our simplification loses accuracy across such a wide range of perturbation. Another possibility is that the dynamics of the chemical model may have been incorrectly interpreted, and the true scaling relationship may be different from the proposed equation. Nonetheless, the agreement between the dynamics observed in the numerical simulation, the chemical system, and blood plasma is surprising. It is particularly interesting that a property of a complex network, such as p_{tr} in blood clotting, can scale over almost three orders of magnitude. There are several possible explanations for this result that may be elucidated by future research: 1), most of the activators of clotting may have similar diffusion coefficients; 2), many of the autocatalytic reaction loops may have similar timescales of reaction; or 3), the timescale of one reaction in the network may be dominant in determining whether initiation occurs or not.

This scaling prediction and future research aimed at providing a better understanding of the threshold response in blood clotting may lead to improved point of care diagnostic tools and drug therapies. Current clinical diagnostic tests, including activated partial thromboplastin time and prothrombin time, do not closely mimic the spatiotemporal dynamics of initiation of clotting in vivo, and a more accurate physical description of clotting could allow the development of improved methods. In addition, the ability to quantify a change in t_r resulting from a change in the dosage of a drug should enable the correct prediction of the potential of a patient's blood to clot at varying doses, and may allow more precise administration of drugs. Of course, some difficulties must be overcome for in vivo application of this scaling prediction, such as reducing spontaneous clotting in whole blood and further characterization of its potential to measure changes in the ability of a patient's blood to clot.

This characterization of the relationship between the timescale of reaction and the critical patch size necessary to initiate a reaction should also be useful for understanding initiation of other autocatalytic systems that demonstrate a threshold response. Understanding dynamics of patches is important, as the clustering of proteins and lipids on membranes maybe a common phenomenon in biological signaling pathways (43,44). Investigating the influence of additional parameters, including transport by convection, changes in boundary conditions, and the effect of a three-dimensional stimulus on initiation will provide a more comprehensive

understanding of the spatiotemporal dynamics of complex, nonlinear systems with patches bearing species involved in autocatalysis and positive feedback loops.

We thank Thuong Van Ha for helpful discussions, Pamela Haltek and Sharice Davis for collecting blood samples, and Jessica M. Price for contributions in editing and writing this article.

This work was supported in part by National Science Foundation CAREER Award No. CHE-0349034 and Office of Naval Research grant No. N000140610630. R.F.I. is a Cottrell Scholar of Research Corporation and an A.P. Sloan Research Fellow. Some of this work was performed at the Materials Research Science and Engineering Center microfluidic facility (funded by the National Science Foundation).

REFERENCES

1. Beltrami, E., and J. Jesty. 2001. The role of membrane patch size and flow in regulating a proteolytic feedback threshold on a membrane: possible application in blood coagulation. *Math. Biosci.* 172:1–13.
2. Diamond, S. L. 2001. Reaction complexity of flowing human blood. *Biophys. J.* 80:1031–1032.
3. Fogelson, A. L., and A. L. Kuharsky. 1998. Membrane binding-site density can modulate activation thresholds in enzyme systems. *J. Theor. Biol.* 193:1–18.
4. Kastrup, C. J., M. K. Runyon, F. Shen, and R. F. Ismagilov. 2006. Modular chemical mechanism predicts spatiotemporal dynamics of initiation in the complex network of hemostasis. *Proc. Natl. Acad. Sci. USA.* 103:15747–15752.
5. Kuharsky, A. L., and A. L. Fogelson. 2001. Surface-mediated control of blood coagulation: the role of binding site densities and platelet deposition. *Biophys. J.* 80:1050–1074.
6. Lobanova, E. S., and F. I. Ataullakhanov. 2003. Unstable trigger waves induce various intricate dynamic regimes in a reaction-diffusion system of blood clotting. *Phys. Rev. Lett.* 91:138301.
7. Runyon, M. K., B. L. Johnson-Kerner, and R. F. Ismagilov. 2004. Minimal functional model of hemostasis in a biomimetic microfluidic system. *Angew. Chem. Int. Ed. Engl.* 43:1531–1536.
8. Ataullakhanov, F. I., and M. A. Panteleev. 2005. Mathematical modeling and computer simulation in blood coagulation. *Pathophysiol. Haemost. Thromb.* 34:60–70.
9. Ataullakhanov, F. I., A. V. Pohilko, E. I. Sinauridze, and R. I. Volkova. 1994. Calcium threshold in human plasma clotting kinetics. *Thromb. Res.* 75:383–394.
10. Jesty, J., J. Rodriguez, and E. Beltrami. 2005. Demonstration of a threshold response in a proteolytic feedback system: control of the autoactivation of Factor XII. *Pathophysiol. Haemost. Thromb.* 34:71–79.
11. van' t Veer, C., and K. G. Mann. 1997. Regulation of tissue factor initiated thrombin generation by the stoichiometric inhibitors tissue factor pathway inhibitor, antithrombin-III, and heparin cofactor-II. *J. Biol. Chem.* 272:4367–4377.
12. Ito, A., Y. Kudo, and H. Oyama. 2005. Propagation and extinction mechanisms of opposed-flow flame spread over PMMA for different sample orientations. *Combust. Flame.* 142:428–437.
13. Bird, R. B., W. E. Stewart, and E. N. Lightfoot. 2002. Transport Phenomena. John Wiley & Sons, New York.
14. Kleinman, L. S., and X. B. Reed. 1995. Interphase mass-transfer from bubbles, drops, and solid spheres—diffusional transport enhanced by external chemical-reaction. *Ind. Eng. Chem. Res.* 34:3621–3631.
15. Feng, J., P. Y. Tseng, K. M. Faucher, J. M. Orban, X. L. Sun, and E. L. Chaikof. 2002. Functional reconstitution of thrombomodulin within a substrate-supported membrane-mimetic polymer film. *Langmuir.* 18: 9907–9913.
16. Esmon, N. L., L. E. Debault, and C. T. Esmon. 1983. Proteolytic formation and properties of γ-carboxyglutamic acid domainless protein-C. *J. Biol. Chem.* 258:5548–5553.
17. Esmon, C. T., and W. G. Owen. 1981. Identification of an endothelial-cell cofactor for thrombin-catalyzed activation of protein-C. *Proc. Natl. Acad. Sci. USA.* 78:2249–2252.
18. Esmon, C. T. 1989. The roles of protein-C and thrombomodulin in the regulation of blood coagulation. *J. Biol. Chem.* 264:4743–4746.
19. Ohno, Y., H. Kato, T. Morita, S. Iwanaga, K. Takada, S. Sakakibara, and J. Stenflo. 1981. A new fluorogenic peptide substrate for vitamin K-dependent blood-coagulation factor, bovine protein-C. *J. Biochem. (Tokyo).* 90:1387–1395.
20. Feistritzer, C., R. A. Schuepbach, L. O. Mosnier, L. A. Bush, E. Di Cera, J. H. Griffin, and M. Riewald. 2006. Protective signaling by activated protein C is mechanistically linked to protein C activation on endothelial cells. *J. Biol. Chem.* 281:20077–20084.
21. Lo, K., and S. L. Diamond. 2004. Blood coagulation kinetics: high throughput method for real-time reaction monitoring. *Thromb. Haemost.* 92:874–882.
22. Rivard, G. E., K. E. Brummel-Ziedins, K. G. Mann, L. Fan, A. Hofer, and E. Cohen. 2005. Evaluation of the profile of thrombin generation during the process of whole blood clotting as assessed by thrombelastography. *J. Thromb. Haemost.* 3:2039–2043.
23. Nagypal, I., and I. R. Epstein. 1986. Systematic design of chemical oscillators. 37. Fluctuations and stirring rate effects in the chlorite thiosulfate reaction. *J. Phys. Chem.* 90:6285–6292.
24. Dorffler-Melly, J., M. de Kruif, L. A. Schwarte, R. F. Franco, S. Florquin, C. A. Spek, C. Ince, P. H. Reitsma, and H. ten Cate. 2003. Functional thrombomodulin deficiency causes enhanced thrombus growth in a murine model of carotid artery thrombosis. *Basic Res. Cardiol.* 98:347–352.
25. Warkentin, T. E. 2003. Management of heparin-induced thrombocytopenia: a critical comparison of lepirudin and argatroban. *Thromb. Res.* 110:73–82.
26. Yu, C. H., A. N. Parikh, and J. T. Groves. 2005. Direct patterning of membrane-derivatized colloids using in-situ UV-ozone photolithography. *Adv. Mater.* 17:1477–1480.
27. Yee, C. K., M. L. Amweg, and A. N. Parikh. 2004. Direct photochemical patterning and refunctionalization of supported phospholipid bilayers. *J. Am. Chem. Soc.* 126:13962–13972.
28. Groves, J. T., and S. G. Boxer. 2002. Micropattern formation in supported lipid membranes. *Acc. Chem. Res.* 35:149–157.
29. Contino, P. B., C. A. Hasselbacher, J. B. A. Ross, and Y. Nemerson. 1994. Use of an oriented transmembrane protein to probe the assembly of a supported phospholipid-bilayer. *Biophys. J.* 67:1113–1116.
30. Galvin, J. B., S. Kurosawa, K. Moore, C. T. Esmon, and N. L. Esmon. 1987. Reconstitution of rabbit thrombomodulin into phospholipid vesicles. *J. Biol. Chem.* 262:2199–2205.
31. Kawabata, S. I., T. Miura, T. Morita, H. Kato, K. Fujikawa, S. Iwanaga, K. Takada, T. Kimura, and S. Sakakibara. 1988. Highly sensitive peptide-4-methylcoumaryl-7-amide substrates for blood-clotting proteases and trypsin. *Eur. J. Biochem.* 172:17–25.
32. Whitesides, G. M., E. Ostuni, S. Takayama, X. Y. Jiang, and D. E. Ingber. 2001. Soft lithography in biology and biochemistry. *Annu. Rev. Biomed. Eng.* 3:335–373.
33. Toner, M., and D. Irimia. 2005. Blood-on-a-chip. *Annu. Rev. Biomed. Eng.* 7:77–103.
34. Atencia, J., and D. J. Beebe. 2005. Controlled microfluidic interfaces. *Nature.* 437:648–655.
35. El-Ali, J., P. K. Sorger, and K. F. Jensen. 2006. Cells on chips. *Nature.* 442:403–411.
36. Tseng, P. Y., S. S. Rele, X. L. Sun, and E. L. Chaikof. 2006. Membrane-mimetic films containing thrombomodulin and heparin inhibit tissue factor-induced thrombin generation in a flow model. *Biomaterials.* 27:2637–2650.
37. Xu, J., N. L. Esmon, and C. T. Esmon. 1999. Reconstitution of the human endothelial cell protein C receptor with thrombomodulin in

phosphatidylcholine vesicles enhances protein C activation. *J. Biol. Chem.* 274:6704–6710.

38. Beltrami, E., and J. Jesty. 1995. Mathematical analysis of activation thresholds in enzyme-catalyzed positive feedbacks—application to the feedbacks of blood coagulation. *Proc. Natl. Acad. Sci. USA.* 92:8744–8748.
39. Mikhailov, A. S., and K. Showalter. 2006. Control of waves, patterns and turbulence in chemical systems. *Phys. Rep. Rev. Sec. Phys. Lett.* 425:79–194.
40. Epstein, I. R., and K. Showalter. 1996. Nonlinear chemical dynamics: oscillations, patterns, and chaos. *J. Phys. Chem.* 100:13132–13147.
41. Toth, A., V. Gaspar, and K. Showalter. 1994. Signal transmission in chemical systems—propagation of chemical waves through capillary tubes. *J. Phys. Chem.* 98:522–531.
42. Balasubramanian, V., E. Grabowski, A. Bini, and Y. Nemerson. 2002. Platelets, circulating tissue factor, and fibrin colocalize in ex vivo thrombi: real-time fluorescence images of thrombus formation and propagation under defined flow conditions. *Blood.* 100:2787–2792.
43. Simons, K., and D. Toomre. 2000. Lipid rafts and signal transduction. *Nat. Rev. Mol. Cell Biol.* 1:31–39.
44. Allen, J. A., R. A. Halverson-Tamboli, and M. M. Rasenick. 2007. Lipid raft microdomains and neurotransmitter signaling. *Nat. Rev. Neurosci.* 8:128–140.